

Cubic Millimeter Power Inductor Fabricated in Batch-Type Wafer Technology

Menouer Saidani and Martin A. M. Gijs

Abstract—A hybrid technology for the realization of three-dimensional (3-D) miniaturized power inductors is presented. Our devices consist of planar Cu coils on polyimide substrates, and mm-size ferrite magnetic cores, obtained by three-dimensional micro-patterning of ferrite wafers using powder blasting. The coils are realized using an in-house developed high-resolution polyimide spinning and Cu electroplating process. Winding widths down to $5\ \mu\text{m}$ have been obtained and total device volumes are ranging between 1.5 and $10\ \text{mm}^3$. Inductive and resistive properties are characterized as a function of frequency; inductance values in the $100\ \mu\text{H}$ range have been obtained. [744]

Index Terms—Electroplating, ferrite, flex-foil, inductor, polyimide, powder blasting.

I. INTRODUCTION

TODAY there is a great demand for miniaturized electronic devices like inductors and transformers, in particular in the field of power electronics, for switched mode power supply applications. High frequency, high-energy density, and high-efficiency power converters, using miniaturized inductors, are required for communication and military/aerospace applications and for use in computer/peripheral or other portable devices. Several examples of micromachined transformers have been reported. For example, Park *et al.* [1] and Ahn *et al.* [2] reported on $4\ \text{mm} \times 1\ \text{mm} \times 0.13\ \text{mm}$ size inductors based on a $15\ \mu\text{m}$ thick electroplated $\text{Ni}_{80}\text{Fe}_{20}$ and $\text{Ni}_{50}\text{Fe}_{50}$ magnetic cores. The structure is realized by a number of sputter deposition, electroplating, photoresist spinning and patterning steps. Inductance values of approximately $0.4 - 0.1\ \mu\text{H}$ were reported at $1\ \text{kHz} - 1\ \text{MHz}$. Löchel *et al.* [3] have used thick resist technology, sputtering and clever electroplating/etching methods to fabricate coils of a few mm size, based on NiFe core material. Inductance values of the order of $1\ \mu\text{H}$ were reported at $125\ \text{kHz}$. These devices were not intended to function as power inductors or transformers: all measurements were done at small primary excitation voltages so that eddy current and magnetic hysteresis losses would be minimized. Microtransformers of $5\ \text{mm}$ size integrated with diodes on an Si wafer were also reported by Mino *et al.* [4], [5]. These transformers are based on an amorphous magnetic core prepared by sputtering, in the form of three separate layers of CoZrRe, each $5\ \mu\text{m}$ thick, with $0.1\ \mu\text{m}$ SiO_2 spacer layers. This layered configuration was chosen exactly to reduce eddy current losses in the magnetic core. Reported inductance values were in

the range of $0.5 - 1\ \mu\text{H}$. A specially configured transformer was realized by Yamasawa *et al.* [6] by sandwiching primary and secondary coils in between two $10\ \mu\text{m}$ thick amorphous CoZr layers. An inductance value of $8.5\ \mu\text{H}$ at $1\ \text{MHz}$ was obtained by this rather large planar device of $40\ \text{mm} \times 30\ \text{mm}$. A spiral coil type thin film microtransformer ($2.4 \times 3.1\ \text{mm}^2$) using RF-sputtered CoNbZr layers, was also proposed by Yamaguchi *et al.* for MHz switching regulators [7].

Besides the development of micromachined inductors, which are mostly based on metallic magnetic materials and which are not primarily intended to function in a power application, also power electronics has been a field of strong miniaturization. An important factor for the size reduction of a power inductor or transformer is its operation frequency (typically $0.1 - 1\ \text{MHz}$), as with increasing frequency, more power cycles can pass the inductive device. These high frequencies necessitate the use of high-resistivity magnetic core materials, such as ferrites, for reducing eddy current losses. During recent years, a large research effort has been developed in the field of so-called planar magnetics, where one integrates flat three-dimensional (3-D) ferrite cores with Cu windings realized in planar Printed Circuit Board (PCB) technology [8]–[10]. In the MEMS field, inductors have been fabricated using screen printed polymer/ferrite layer composites, and inductances in the $0.5 - 1.5\ \mu\text{H}$ range have been achieved [11], [12]. Here, fine ferrite particles are introduced into a polyimide matrix to form a composite. We have recently proposed a batch-type solution for the fabrication of 3-D inductors, where we combined micromachined E-shaped magnetic ferrite cores with planar Cu coils, realized using commercially available flex-foil technology [13]. The commercial technology is based on the gluing of thin Cu foils on a polyimide substrate and their subsequent micropatterning in a wet etching process. Due to Cu foil/polyimide detachment problems and mask underetching effects, a minimum winding width $w = 25 - 30\ \mu\text{m}$ and a winding pitch $p = 50 - 60\ \mu\text{m}$ is feasible (see for example ref. [14]). Clearly, this minimum dimension presents a strong limit to the extreme miniaturization of inductive devices, as the inductance value scales with the square of the number of windings that can be fitted into a given inductor volume.

In this paper, we present a new process for the microfabrication of multilayered Cu coils on a flexible polyimide (Kapton) substrate. The technique involves various lithography, polyimide spinning, Cu electroplating, planarization and plasma etching steps. For mechanical support during processing, the Kapton substrate is temporarily glued on an easy removable Si wafer. This Si wafer technology based process has the potential to realize a winding thickness $t = 5\ \mu\text{m}$, a minimum winding width $w = 5\ \mu\text{m}$ and a minimum winding pitch

Manuscript received August 23, 2001; revised September 9, 2002. Subject Editor K. D. Wise.

The authors are with the Institute of Microelectronics and Microsystems, School of Engineering Sciences and Techniques of the Swiss Federal Institute of Technology Lausanne, Switzerland.

Digital Object Identifier 10.1109/JMEMS.2002.807472

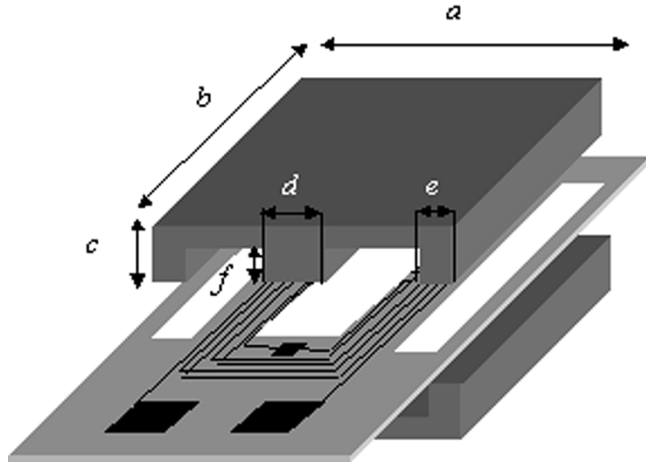


Fig. 1. Perspective view of a double layered planar coil on a polyimide substrate assembled with two ferrite E-cores.

$p = 15 \mu\text{m}$. These high-resolution coils are combined with extremely miniaturized E-shaped ferrite cores. The latter are microstructured out of mm-thick ferrite wafers using a high pressure eroding powder beam ($30 \mu\text{m}$ alumina particles), and various metal contact masks [15]. The technique has the potential to realize many cores in parallel and assemble them at wafer-level with the electrical winding patterns. Hereafter, complete devices are separated. Thanks to precise alignment and overlay of the metal contact masks, we can micropattern 3-D shapes in the ferrite typically down to a few $100 \mu\text{m}$ and with a resolution of the order of the powder particle size. By combining the extremely miniaturized cores with our high resolution flex-foil process for the electrical coils, we are able to realize power inductors in the $1\text{--}10 \text{mm}^3$ volume range with unprecedentedly high inductance values (up to $100 \mu\text{H}$ for a double layered coil) for the given inductor volumes. A ‘power’ inductive device can operate at high input voltages and at high frequencies ($1\text{--}10 \text{MHz}$) with minimum losses. Special ferrite materials (like the Philips 3F3 material we use) have been developed, characterized by a high resistivity and low magnetic hysteresis. We have exactly chosen for such ‘power ferrite’ for our devices, so that the magnetic losses of the inductive device are minimized, even at high frequencies.

II. DESIGN

Fig. 1 shows a conceptual view of the hybrid magnetic device which is composed of a set of magnetic E-cores and a double layered coil on a polyimide substrate. A spiral inductor design is considered for the realization of the windings due to its simplicity of fabrication and the potential of realizing large inductance values. The inductor coil is composed of two conducting layers connected through a $200 \mu\text{m}$ large square via and fully encapsulated in polyimide.

The geometrical dimensions of the magnetic cores are obtained by scaling-down the design from ordinary macroscopic Philips planar E-cores [16]. Depending on this scaling factor, three E-core structures are designed and fabricated with the dimensions listed in Table I.

We have realized three types of ferrite cores. The parameters a , b , c , d , e and f in Table I correspond to the scheme of Fig. 1

TABLE I
CORE DESIGN PARAMETERS (SEE Fig. 1)

core	a (mm)	b (mm)	c (mm)	d (mm)	e (mm)	f (mm)	A_L (nH)
1	4	1.43	1	0.86	0.43	0.57	450
2	3	1.04	0.75	0.64	0.32	0.43	340
3	2	0.71	0.5	0.44	0.22	0.28	230

and represent the length, the width, the thickness, the center leg and lateral leg widths and the depth of each core, respectively. A_L represents the calculated inductance factor for each core design and it is defined by relation (2). An optimized design is obtained, when having a minimum ferrite volume for a given magnetic flux. In practice, this is obtained when the cross sections for the magnetic flux : $d \times b = 2(e \times b)$ and $b \times e = (c - f) \times b$.

Ferrite cores are attractive and very suitable for magnetic power applications. This is due to two reasons: first, high relative permeability factors ($\mu_r \sim 2000$) allow to obtain high inductance values with minimal number of turns; secondly, the high resistivity ($\rho \sim 1 - 10^5 \Omega - \text{cm}$) reduces eddy currents losses at high frequency. The inductance value of an inductor can be simply expressed in terms of the inductance factor A_L of the magnetic core and the number of windings N by [16]

$$L = A_L N^2 \quad (1)$$

The factor A_L contains the geometrical and magnetic properties of the ferrite core through the following relation:

$$A_L = \frac{\mu_0 \mu_e}{\sum \frac{l_e}{A_e}} \quad (2)$$

where A_e and l_e are, respectively, the cross-sectional area and the path length of the core, and μ_e is the effective permeability which takes into account the eventual presence of an air gap in a closed magnetic circuit.

For small air gaps, relation (3) makes a quantitative link between the initial permeability of the material μ_i , the air gap length l_g , and the effective path length of the magnetic circuit l_e :

$$\mu_e = \frac{\mu_i}{1 + \frac{l_g \mu_i}{l_e}} \quad (3)$$

The air gap l_g is composed of an intentionally fabricated one and a spurious one, originating from the surface roughness of the ferrite material (in the $0.5\text{--}1.0 \mu\text{m}$ range). Air gaps in macroscopic cores are typically of the order of a few tens micrometers in magnitude. When scaling down this design, consequently, the influence of roughness on the effective permeability will be more important for miniaturized E-cores. The problem of roughness can be solved by using polished ferrite wafers and by applying a strong clamping force when assembling the two E-cores.

III. FABRICATION PROCESS

A. Magnetic Cores

For the magnetic cores, we use high relative permeability ($\mu_r = 1800$) 3F3 ferrite wafers of Philips. The three types of three-dimensional ferrite E-cores are micromachined in 1-mm,

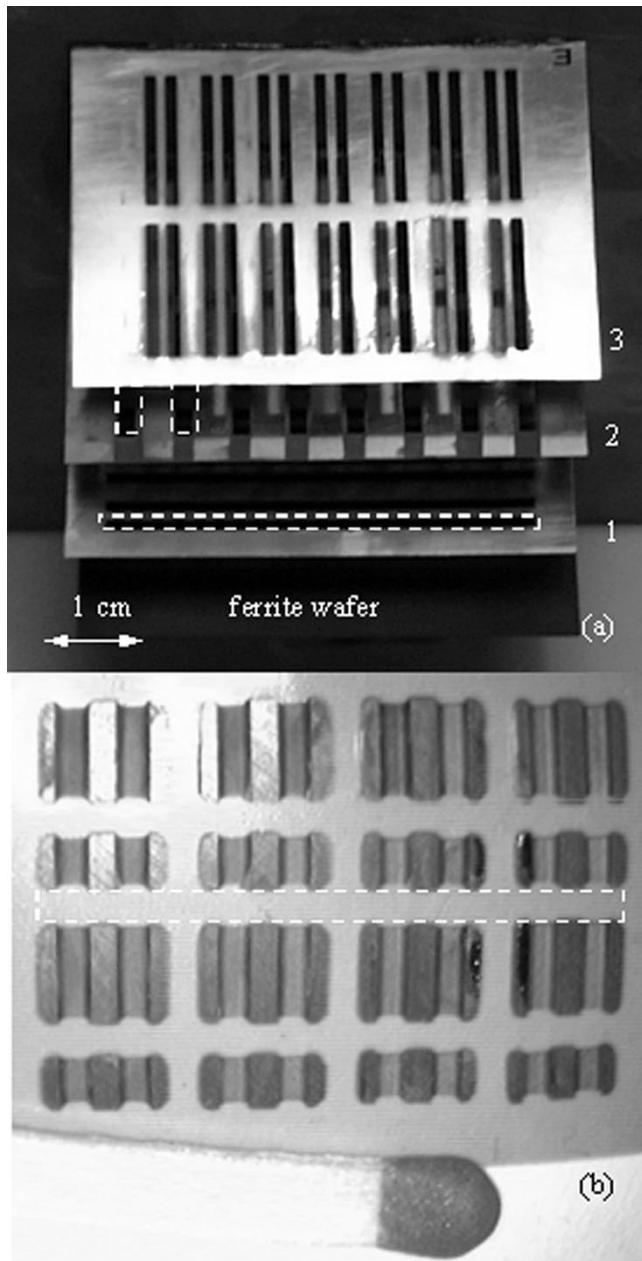


Fig. 2. (a) Successive used powder blasting masks. (b) Array of structured ferrite E-cores, powder blasted in a ferrite wafer. The dashed line in Fig. 2(b) represents schematically the position of the longitudinal hole, as present in mask 1 of Fig. 2(a).

0.75-mm, and 0.5-mm-thick ferrite wafers using mechanical micro-erosion by powder blasting [15]. Three 0.5-mm-thick stainless steel masks, shown in Fig. 2(a), are subsequently used to realize E-cores like shown in Fig. 2(b). During the powder blasting process, these masks are temporarily glued to the ferrite wafer to promote the mechanical contact and to prevent underetching effects. By performing an x- and y-axis translation of the powder blasting nozzle, we obtain a uniform exposure of the fixed ferrite wafer. An example of an array of ferrite cores, after fabrication and gluing on blue tape, is shown in Fig. 2(b).

Fig. 3 is a scanning electron microscope (SEM) photograph of one of the smallest fabricated single E-cores.

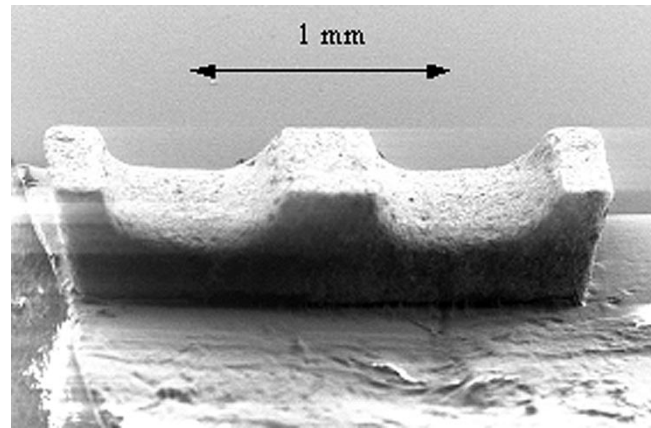


Fig. 3. SEM photograph of the smallest microstructured single ferrite E-core (2 mm \times 0.71 mm \times 0.5 mm).

B. Coils

Presently, standard available flex-foil technology is resolution-limited to structures with a Cu width $w = 25 - 30 \mu\text{m}$ and a winding pitch $p = 50 - 60 \mu\text{m}$. To enable higher densities, we have elaborated a new flex-foil process, which takes advantage of standard clean room wafer-based microfabrication techniques. This process, the sequence of which is shown in Fig. 4, starts with a Si substrate (for mechanical support), which is laminated with a $12.5 \mu\text{m}$ thick polyimide (Kapton) foil, using $12.5 \mu\text{m}$ acrylic adhesive tape. To planarize the surface, a thin layer ($7 \mu\text{m}$ after cure) of liquid polyimide (PI2611 from Dupont) is spun on the top of the Kapton layer after application of an adhesion promoter (VM651 from Dupont).

After coating, the polyimide is cured in nitrogen in a programmable oven (1 h at 150°C , followed by 1 h at 200°C). According to Dupont PI2610 series information, a high temperature cure (300°C) is required to completely dissociate the carrier solvent, fully imidize the film and complete polymer orientation; however, there is sufficient thermal energy at 200°C to nearly complete the polyimide imidization process [17]. This cure at 200°C was chosen to protect the lower Kapton layer from excessive heating.

Then, a 20-nm Cr layer is deposited on the planarized surface to promote adhesion of a subsequent 200 nm Cu seed layer to the polyimide for electroplating. An $8\text{-}\mu\text{m}$ -thick layer of Shipley SJR5740 photoresist is then spun on, exposed with mask 1 and developed to form moulds for the lower part of the windings. The thickness of the photoresist was slightly larger than the thickness of the conductors to ensure that the plating did not extend above the top of the resist layer. After the Cu is given a 10 s etch in 10% sulfuric acid to clean the surface, the moulds are filled with electroplated Cu using standard electroplating techniques (250 g/l of $\text{CuSO}_4 - 5\text{H}_2\text{O} + 25 \text{ ml/l}$ of H_2SO_4 solution). Subsequently, the resist is stripped and the Cu seed layer is removed using a ferric ammonium sulfate solution (40 g/l of $\text{HFeNO}_3\text{S}_2 + 50 \text{ ml/l}$ of H_2SO_4), followed by removal of the chromium adhesion layer in a solution of permanganate of potassium and tri-basic sodium phosphate (80 g/l of $\text{KMnO}_4 + 200 \text{ g/l}$ of Na_3PO_4), giving the structure of Fig. 4(a).

One layer of polyimide is then spun and cured to isolate the Cu windings [see Fig. 4(b)]. After this step the topography of the

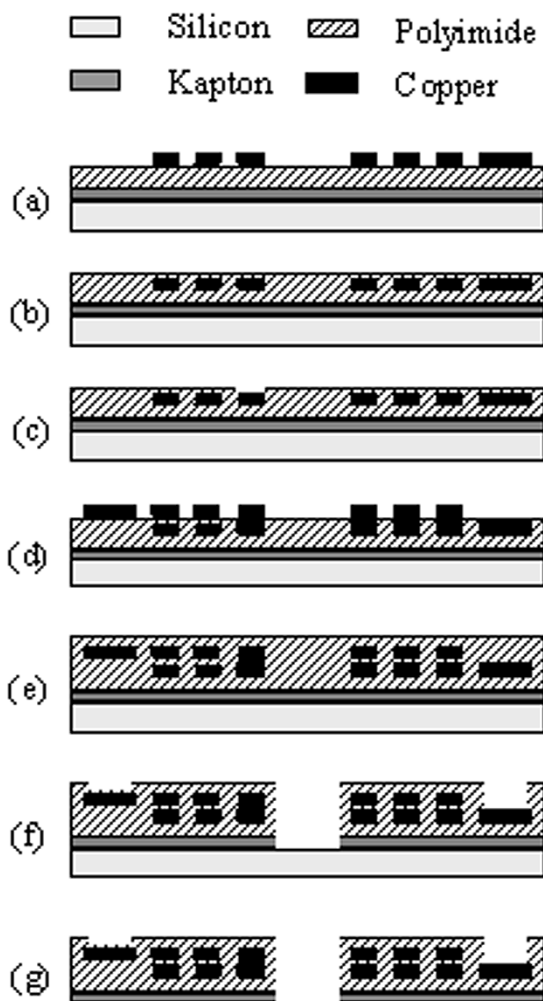


Fig. 4. Fabrication sequence for high-resolution polyimide-based double layered coils on flexible Kapton support: (a) electroplating of the first layer of the coil, (b) polyimide isolation layer deposition, (c) via hole etching, (d) electroplating of the second layer of the coil, (e) polyimide isolation layer deposition, (f) feed-through hole and contact path holes etching (g) final separation of the flexible structures from the Si substrate.

surface was not flat and did not allow high-resolution patterning of the next level. Therefore, using an $0.05 \mu\text{m}$ silica slurry, a chemical-mechanical polishing (CMP) procedure, the parameters of which are listed in Table II, is used for planarization of the polyimide surface.

The wavy topography of the surface (with an amplitude of $1\text{--}2 \mu\text{m}$) is removed in this stage of polishing. An O_2 plasma etch is used to bring the dielectric to a thickness around $1 \mu\text{m}$ from the top of the first electroplated Cu layer, thereby facilitating the via connection to the second layer. Via holes are patterned by using a 800 nm thick PECVD SiO_2 masking layer and an O_2 plasma (the plasma O_2 etching rate is $1 \mu\text{m}/\text{min}$, with a selectivity higher than 1000 with respect to the SiO_2 mask). Hereafter, the silicon oxide mask is removed using wet etching [see Fig. 4 (c)].

From this point, fabrication continues with the next level of windings by depositing a new seed layer on the planarized surface and by repeating the sequence of steps described before [see Fig. 4(d)].

TABLE II
PARAMETERS OF THE CMP PROCESS OF POLYIMIDE

Wafer and Platen speed	15 rpm
Pressure	1 bar
Slurry feed rate	150 ml/min
Slurry composition	silica particles, $0.05 \mu\text{m}$, pH 10
Removal rate	$\sim 300 \text{ nm}/\text{min}$

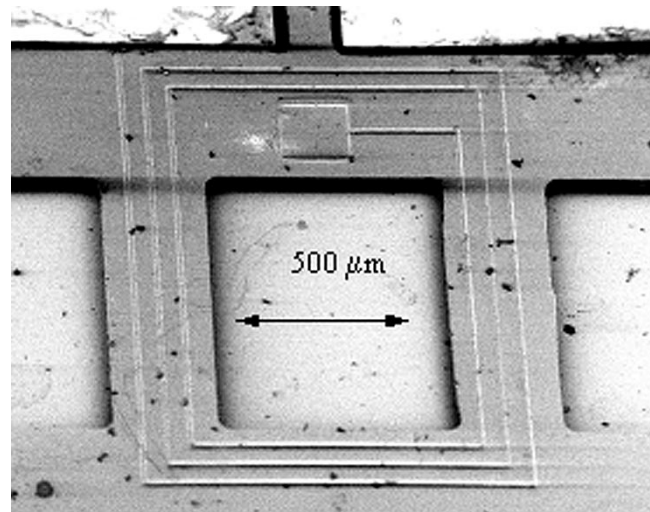


Fig. 5. SEM photograph of the final microfabricated coil on the silicon substrate showing the through-holes for the positioning of the E-cores and the contact paths holes (winding width $w = 20 \mu\text{m}$ and winding pitch $p = 50 \mu\text{m}$).

After removal of the second seed layer, a polyimide passivation layer is applied and cured to protect the top of the windings from oxidation [see Fig. 4(e)]. Finally a silicon oxide mask is deposited and the polyimide is etched in an O_2 plasma to create the through-holes for the positioning of the E-cores and to clear the contact paths [see Fig. 4(f)]. To separate the flexible structures from the Si substrate, a bath of acetone is used to remove the adhesive between the Kapton film and the wafer [see Fig. 4(g)].

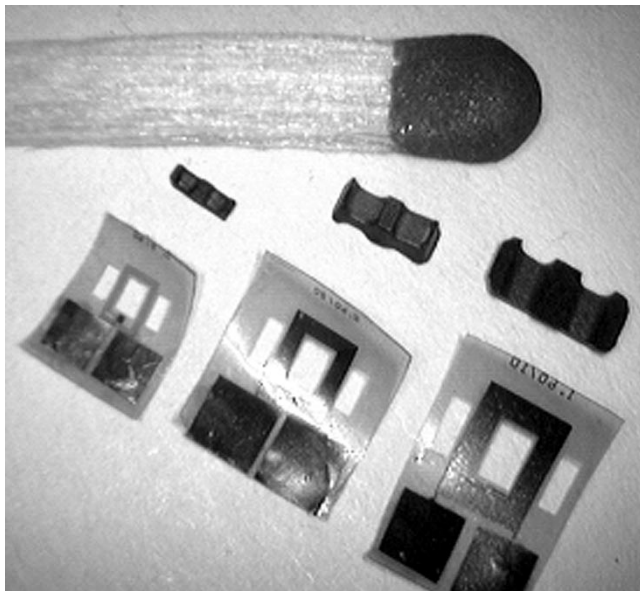
Fig. 5 shows a finished coil which consists of two layers of Cu windings with a line width $w = 20 \mu\text{m}$, a line pitch $p = 50 \mu\text{m}$, and a number of turns $N = 6$, fully encapsulated in polyimide PI2611 on a flexible Kapton film substrate. The total thickness of the coil is $45 \mu\text{m}$.

Fig. 6(a) is a photograph of the three sizes of coils we realized, with their respective ferrite cores. Fig. 6(b) is a photograph of an assembled inductor of the smallest type. The flexible coils and the E-cores are assembled, whereby the two E-cores auto-align as a consequence of minimization of magnetic demagnetization energy. The E-cores are then glued together to reduce air gap, they are also mechanically clamped.

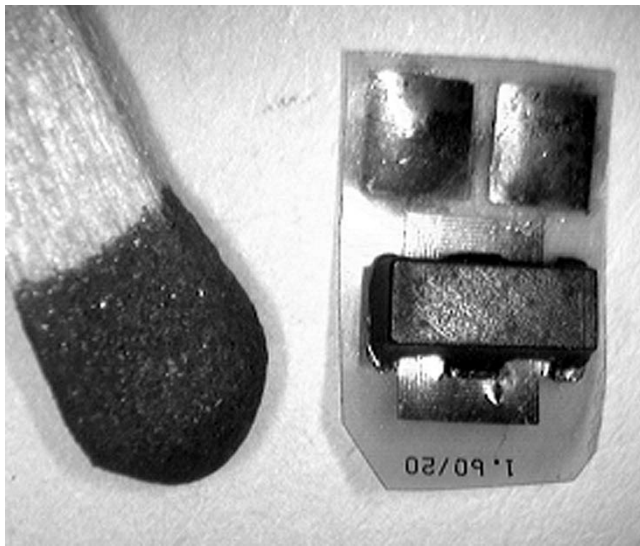
IV. ELECTRICAL CHARACTERIZATION

Table III lists a set of four inductors, based on the first type of ferrite core of Table I, assembled with coils of various number of windings N .

The electrical properties of these samples are measured using a Hewlett Packard 4194A impedance/gain-phase ana-



(a)



(b)

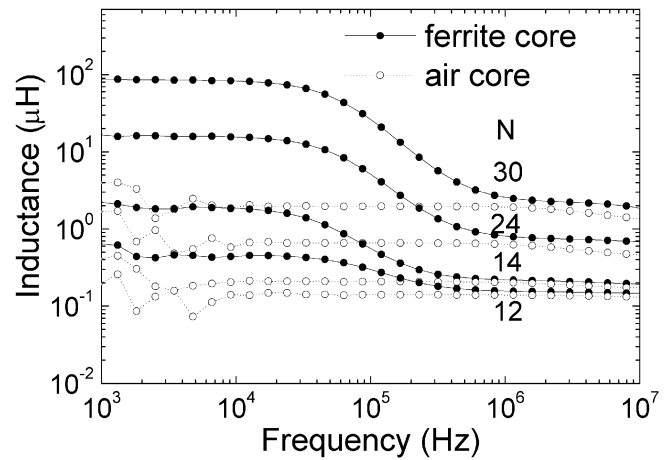
Fig. 6. (a) Photograph of flex-foil coils of various sizes, with their respective ferrite cores. (b) Final assembled inductor.

TABLE III
PARAMETERS OF THE MEASURED COILS

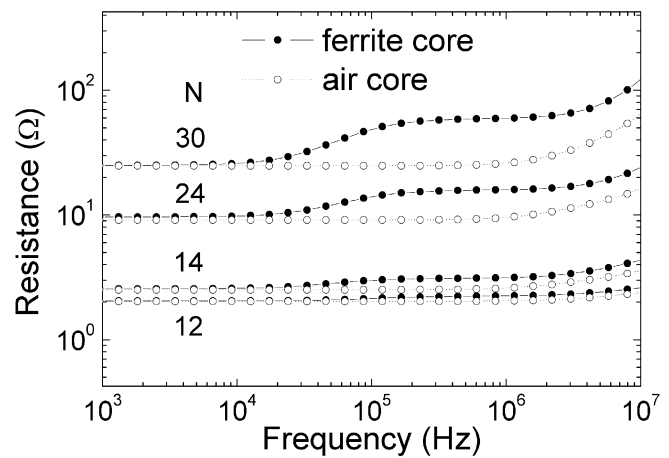
Coil number	w (μm)	p (μm)	N
1	30	130	12
2	60	100	14
3	50	60	24
4	40	50	30

lyzer. Using a logarithmic frequency sweep between 10^3 and 10^7 Hz with a sinusoidal signal level of 500 mV rms, inductance and resistance are recorded as a function of frequency.

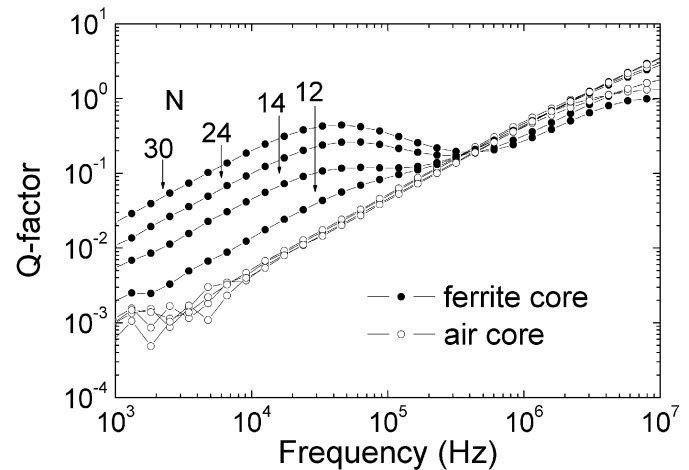
Fig. (7a) and (7b) show inductance and resistance measurements, respectively of each device as a function of frequency, with and without the application of the ferrite cores and with the number of windings N as a parameter. One clearly sees the strong enhancement of the inductance due to the presence of the



(a)



(b)



(c)

Fig. 7. Dependence of (a) the inductance, (b) the resistance, and (c) the quality factor on frequency for the selected coils of Table III with various number of windings N , without and with ferrite core.

ferrite. The drop of the inductance in the 0.1–1 MHz range is due to the dependence of the permeability of the magnetic core on frequency [18], but is probably also affected by interwinding capacitance effects.

The “noisy” low-frequency signal (at around 10^3 Hz) for the inductors with the smallest inductance value has its origin in

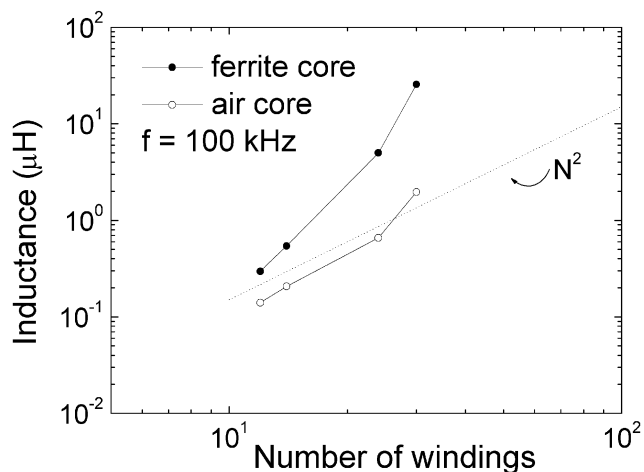


Fig. 8. Power-law dependence of the inductance on the number of windings N at 100 kHz, without and with ferrite core.

the noise limitations of our measurement setup. Indeed, inductive voltages ($2\pi fL$) easily are of the same order of magnitude as thermal noise voltages in this frequency range. As a consequence, a longer sampling time for the measurement can smooth out the measured low-frequency variations in L . The small tumbling of some of the smaller inductances at low frequencies probably is an instrumental measurement error. Resistance increases in the 0.1–1 MHz range due to the increasing magnetic and winding losses at high frequencies. Such behavior is typical when using a power ferrite material like 3F3. If we would have used, for example, a low-resistivity metallic magnetic core material, we would generate at much lower frequencies already significant eddy current losses and important device heating. The significance of our technology is that we can use and microstructure the power ferrite materials without degrading them, and, hence, benefit maximally from their bulk properties, which have been optimized for power applications.

Fig. 7 (c) is a plot of the frequency-dependence of the quality factor $\omega L(\omega)/R(\omega)$, derived from Fig. 7 (a) and (b), for the samples with and without ferrite cores. Without the cores, the quality factor increases about linearly with frequency, but is expected to decrease at still higher frequencies due to the enhancement of resistive losses $R(\omega)$. When using ferrite cores, the quality factor is increased below 0.3 MHz, basically due to the enhancement of L . At still higher frequencies interwinding capacitance effects are gradually shorting out the inductance and the quality factor drops to the value without ferrite core. Typical self-resonant frequencies of our devices are around 200 MHz.

Fig. 8 is a double logarithmic plot of the inductance as a function of the number of windings N at $f = 100$ KHz. Without the ferrite core, we find the typical N^2 power law behavior. The choice for logarithmic axes was made, as the exponent of any power law function (a straight line on this kind of graph) is directly observable from the slope. For an inductor with assembled ferrite core, we observe a deviation of the N^2 behavior which we attribute to variations in parasitic air gaps, core clamping, and capacitive coupling effects between the electrical windings and between the windings and the core. This observation makes it difficult to determine the exact value of the core constant A_L , and hence the permeability, using equa-

tion (1). We verified that at very low frequencies (around 100 Hz), where capacitive coupling effects are minimum, the permeability value is consistent with the value reported for the bulk 3F3 material ($\mu_r \sim 1800$).

V. CONCLUSION

We have developed a high-resolution flex-foil process and combined it with an original way of fabricating miniaturized E-cores from ferrite wafers to realize inductors in the mm^3 volume range. We have measured the electrical properties of these devices as a function of frequency and demonstrated inductance values in the 100 μH range up to 0.1 MHz in frequency.

ACKNOWLEDGMENT

The authors would like to express their thanks to Dr. E. Bornand and M. Farid Amalou for valuable discussions, and the EPFL Center of Microtechnology (CMI) staff for fabrication assistance.

REFERENCES

- [1] J. Y. Park and M. G. Allen, "A comparison of micromachined inductors with different magnetic core materials," in *Proc. IEEE 46th Electronic Components and Technology Conference*, Orlando, FL, 1996, pp. 375–381.
- [2] C. Ahn, Y. Kim, and M. G. Allen, "A comparison of two micromachined inductors (bar and meander type) for fully integrated boost dc/dc power converters," *IEEE Trans. Power Electron.*, vol. 11, pp. 239–245, 1996.
- [3] B. Löchel, A. Maciossek, M. Rothe, and W. Windbracke, "Microcoils fabricated by UV depth lithography and galvanoplatin," *Sens. Actuators, Phys. A*, vol. 54, pp. 663–668, 1996.
- [4] M. Mino, T. Yachi, A. Tago, K. Yanagisawa, and K. Sakakibara, "Planar microtransformer with monolithically integrated rectifier diodes for micro-switching converters," *IEEE Trans. Magn.*, vol. 32, pp. 291–296, 1996.
- [5] T. Yachi, M. Mino, A. Tago, K. Yanagisawa, and K. Sakakibara, "A new planar microtransformer for use in micro-switching converters," *IEEE Trans. Magn.*, vol. 28, pp. 1969–1973, 1992.
- [6] K. Yamasawa, K. Maruyama, I. Hirohama, and P. P. Biringer, "High frequency operation of a planar-type microtransformer and its application to multilayered switching regulators," *IEEE Trans. Magn.*, vol. 26, pp. 1204–1209, 1990.
- [7] K. Yamaguchi, E. Suguwara, O. Nakajima, and H. Matsuki, "Load characteristics of a spiral coil type thin film microtransformer," *IEEE Trans. Magn.*, vol. 29, pp. 3207–3209, 1993.
- [8] D. van der Linde, C. A. M. Boon, and J. B. Klaassens, "Design of a high-frequency planar power transformer in multilayer technology," *IEEE Trans. Ind. Electron.*, vol. 38, pp. 137–141, 1991.
- [9] S. Ben-Yaakov, *The Benefits of Planar Magnetics in HF Power Conversion*. Rishon-Le Zion, Israel: Payton.
- [10] N. Dai, A. W. Lofti, G. Skutt, W. Tabisz, and F. C. Lee, "A comparative study of high-frequency, low-profile planar transformer technologies," in *Proc. IEEE 9th Applied Power Electronics Conference and Exposition*, 1994, pp. 226–232.
- [11] J. Y. Park and M. G. Allen, "Low temperature fabrication and characterization of integrated packaging-compatible, ferrite-core magnetic devices," in *Proc. IEEE 12th Applied Power Electronics Conference and Exposition*, vol. 1, 1997, pp. 361–367.
- [12] J. Y. Park, L. K. Lagorce, and M. G. Allen, "Ferrite-based integrated planar inductors and transformers fabricated at low-temperature," *IEEE Trans. Magn.*, vol. 33, pp. 3322–3324, 1997.
- [13] F. Amalou, E. L. Bornand, and M. A. M. Gijs, "Batch-type millimeter-size transformers for miniaturized power applications," *IEEE Trans. Magn.*, vol. 37, pp. 2999–3003, 2001.
- [14] Dyconex. Product Information. [Online]www.dyconex.com
- [15] E. Belloy, S. Thurre, E. Walckiers, A. Sayah, and M. A. M. Gijs, "The introduction of powder blasting for sensor and microsystem applications," *Sens. Actuators, Phys. A*, vol. 84, pp. 330–337, 2000.

- [16] *Philips Catalogue, Magnetic Products*, Soft Ferrites, 1999.
- [17] PI2610 Series—Product Information and Process Guidelines. [Online] www.hdmicrystems.com
- [18] J. Y. Park and M. G. Allen, "Integrated electroplated micromachined magnetic devices using low temperature fabrication processes," *IEEE Trans. Elect. Packag. Manuf.*, vol. 23, pp. 48–55, 2000.



Menouer Saidani received the degree in materials science from the University of Science and Technology Houari Boumedienne of Algiers in 1992. In January 2000, he received the Magister degree in theoretical physics from the same university on his study of the bulk and surface magnetization in $\text{Fe}_x\text{Ni}_{1-x}$ alloys.

He is now with the Institute of Microelectronics and Microsystems at the Federal Institute of Technology Lausanne (EPFL) as a Research Assistant and he is currently working on development of hybrid miniaturized inductors and transformers.



Martin A.M. Gijs received the degree in physics in 1981 from the Katholieke Universiteit Leuven, Belgium, and the Ph.D. degree in physics at the same university in 1986.

He joined the Philips Research Laboratories, Eindhoven, The Netherlands, in 1987. Subsequently, he has worked there on micro- and nanofabrication processes of high-critical temperature superconducting Josephson and tunnel junctions, the microfabrication of microstructures in magnetic multilayers showing the giant magnetoresistance effect, the design and realization of miniaturized motors for hard disk applications, and the design and realization of planar transformers for miniaturized power applications. He joined the Swiss Federal Institute of Technology Lausanne (Ecole Polytechnique Fédérale de Lausanne) in 1997. Currently, he is Professor in the Institute of Microelectronics and Microsystems, where he is responsible for the Microsystems Technology group. His main interests are in developing technologies for novel inductive-type devices, new microfabrication technologies for microsystems fabrication, in general, and the development and use of microsystems technologies for biomedical applications, in particular.